

The Redshift-Space Two Point Correlation Function of ELAIS-S1 Galaxies

V. D’Elia,¹ E. Branchini,² F. La Franca,² V. Baccetti,² I. Matute,³
F. Pozzi,⁴ C. Gruppioni⁵

¹INAF-Osservatorio Astronomico di Roma via Frascati 33, Monteporzio-Catone (RM), I-00040 Italy

²Dipartimento di Fisica, Università degli Studi “Roma Tre”, Via della Vasca Navale 84, I-00146, Roma, Italy

³Max-Planck Institut für extraterrestrische Physik (MPE), Giessenbachstrasse, Postfach 1312, 85741 Garching, Germany

⁴Dipartimento di Astronomia, Università di Bologna, viale Berti Pichat 6, I-40127 Bologna, Italy

⁵INAF-Osservatorio Astronomico di Bologna, via Ranzani 1, I-40127 Bologna, Italy

Released 2005 January 14

ABSTRACT

We investigate the clustering properties of galaxies in the recently completed ELAIS-S1 redshift survey through their spatial two point autocorrelation function. We used a sub-sample of the ELAIS-S1 catalog covering approximately 4 deg^2 and consisting of 148 objects selected at $15\mu\text{m}$ with a flux $> 0.5\text{ mJy}$ and redshift $z < 0.5$. We detected a positive signal in the correlation function that, in the range of separations $1 - 10\ h^{-1}\text{Mpc}$ is well approximated by a power law with a slope $\gamma = 1.4 \pm 0.25$ and a correlation length $s_0 = 5.4 \pm 1.2\ h^{-1}\text{Mpc}$, at the 90 % significance level. This result is in good agreement with the redshift-space correlation function measured in more local samples of mid infrared selected galaxies like the IRAS PSCz redshift survey. This suggests a lack of significant clustering evolution of infrared selected objects out to $z = 0.5$ that is further confirmed by the consistency found between the correlation functions measured in a local ($z < 0.2$) and a distant ($0.2 < z < 0.5$) subsample of ELAIS-S1 galaxies. We also confirm that optically selected galaxies in the local redshift surveys, especially those of the SDSS sample, are significantly more clustered than infrared objects.

Key words: galaxies: clusters: general - galaxies: evolution - cosmology: observation - Large scale structure of Universe - infrared: galaxies

1 INTRODUCTION

Investigating the redshift-space distribution of galaxies has long been regarded as a fundamental aspect of observational cosmology. The primary statistical tool for characterizing galaxy clustering is the spatial two point correlation function, $\xi(s)$ since, in the current paradigm of structure formation, the galaxy two-point correlation function is directly related to the initial power spectrum of mass density fluctuations.

This is true as long as galaxies trace the underlying mass density field. However, it is now well established that the clustering of galaxies at low redshift depends on a variety of factors, implying that not all types of galaxies can be regarded as unbiased mass tracers. The clustering of optically selected galaxies has been found to depend on galaxy luminosity (Norberg *et al.* 2002 and reference therein), morphological and spectral type (Hermit *et al.* 1996, Zehavi *et al.* 2002, Magdwick *et al.* 2003). On the other hand, the clustering of infrared selected galaxies seems to depend on

their infrared color (Hawkins *et al.* 2001) rather than on luminosity (Szapudi *et al.* 2000).

The evidence that different galaxy populations might give different biased pictures of the mass distribution has complicated but also enriched the interpretation of galaxy clustering. Indeed, the very fact that the spatial clustering of galaxies is related to their physical properties represents an important observational test for all theories of galaxy formation. In particular, strong constraints on galaxy evolution models can be obtained by measuring the relative clustering of different extragalactic objects as a function of redshifts, for which very deep galaxy samples are required.

Several deep redshift surveys of optically selected galaxies, like the Keck surveys of the GOODS-north (Wirth *et al.* 2004) and GOODS-south (Vanzella *et al.* 2004) fields and the DEEP2 redshift survey (Davis *et al.* 2003), are currently being performed. First results based on early data look very promising indeed. The analysis of Coil *et al.* (2004) has shown that the two-point correlation function of DEEP2 galaxies with a median redshift $z = 1.14$ is consistent with

that measured by Adelberger *et al.* (2003) in a very deep ($z \sim 3$) sample of Lyman break galaxies but is significantly smaller than the correlation measured in the local ($z \sim 0$) 2dF galaxy sample. Since 2dF b_j -selected galaxies are known to trace the underlying mass density field in an unbiased way (Verde *et al.* 2002, Lahav *et al.* 2002), the smaller correlation measured in DEEP2 survey implies that this is not a strongly biased sample of objects either, since the clustering of the dark mass is expected to decrease with redshift in a similar way (Coil *et al.* 2004).

Mid-infrared selected galaxies also constitutes a very interesting population of objects since they are also known to trace the underlying mass distribution in the local universe in an almost unbiased fashion. More precisely, it has been found that the fluctuations in their number density, δ_g is related to the underlying mass overdensity field δ_m through a simple, linear biasing relation $\delta_g \sim 1.2\delta_m$ (Tegmark, Zaldarriaga & Hamilton 2001 and Taylor *et al.* 2002). Another reason why mid-infrared selection is interesting is that luminosity in this band is approximately proportional to star-formation rate (independent of dust), thus a mid-infrared sample of galaxies will highlight the distribution of star-formation activity at a particular epoch. Clearly, it would be very important to quantify the clustering evolution of mid-infrared selected objects and compare it with that of optically selected galaxies. This is indeed the main goal of this work in which we analyze the clustering properties of sample of mid-infrared selected galaxies extracted from the ELAIS redshift survey (Oliver *et al.* 2000) and extending out to a redshift $z = 0.5$. According to La Franca *et al.* (2004), two main spectroscopic classes have been found to dominate the extragalactic population of these objects: star-forming galaxies (from absorbed to extreme starbursts: $\nu L\nu(15\mu m) \sim 10^8 - 10^{11} L_\odot$), which account for 75% of the sources, and active galactic nuclei (excluded from this analysis) which account for 25% of the sources. About 20% of the extragalactic ELAIS sources are dust-enshrouded starburst galaxies, while passive galaxies are essentially absent from the sample.

Our analysis is performed in redshift-space and thus complements the previous work of Gonzalez-Solares *et al.* (2004) who measured the angular correlation properties of a similar sample of ELAIS galaxies that from which they have inferred their spatial correlation properties.

The outline of this paper is as follows. In section 2 we describe the ELAIS-S1 galaxy redshift survey that we analyze in this work. In section 3 we discuss our method of estimating the two-point correlation function, assess its robustness and evaluate its statistical uncertainties. The main results are presented in section 4, and discussed in section 5, in which we also draw our main conclusions.

2 THE ELAIS S1 SAMPLE

The European Large-Area *ISO* survey (ELAIS, Oliver *et al.* 2000; Rowan-Robinson *et al.* 2004) is the largest Open Time programme conducted by the *ISO* satellite (Kessler *et al.* 1996). It covers an area of 12 deg^2 , divided in four fields (N1, N2 and N3 in the northern hemisphere and S1 in the southern one) distributed across the sky in order to decrease the biases due to cosmic variance. The survey bands

are at 6.7, 15, 90 and $170\mu m$; the $15\mu m$ one presents the highest density of galaxies (Serjeant *et al.* 2000, Gruppioni *et al.* 2002, La Franca *et al.* 2004), making it the best choice for a study of their clustering properties. In this work we concentrate on the southern area, S1.

This survey is made of nine raster observations, each covering $40 \times 40 \text{ arcmin}^2$. The final analysis catalog at $15 \mu m$ in the S1 field has been released by Lari *et al.* (2001) covering an area of $2 \times 2 \text{ deg}^2$ centered at $\alpha(2000) = 00^h 34^m 44.4^s$, $\delta(2000) = -43^\circ 28' 12''$. It includes 462 mid-IR sources down to a flux limit of 0.5 mJy. We have restricted our analysis to a highly reliable subsample of 406 objects (La Franca *et al.* 2004).

A detailed description of the optical classification of the ELAIS-S1 sources, size and completeness function of the areas used in our study, as well as the observed counts for each class of sources (normal galaxies, Starburst galaxies and AGN) are presented by La Franca *et al.* (2004). The measure of the evolution of star-forming galaxies has been investigated by Pozzi *et al.* (2004) and Gruppioni *et al.* (2005), while a first estimate of the luminosity function for type-1 AGN has been presented by Matute *et al.* (2002)¹.

The central raster, S1_R5, has been observed three times and thus represents the deepest part of the sample. As a consequence the ELAIS-S1 area has been divided into two regions: a) the central and deepest part (S1_R5) which covers 0.55 deg^2 and reaches a 20% completeness at fluxes of 0.7 mJy, and b) the remaining area (S1_Rest) which covers 3.65 deg^2 and reaches a 20% completeness at fluxes of 1.1 mJy.

The optical analysis of the 406 objects brings 332 (80%) optical identification on CCD exposures down to $R \sim 23$, and 290 spectroscopic classifications (90% of the optically identified sample). Of these, 93 were found to be stars and 199 extragalactic sources. Among these, we kept only the galaxies with $z < 0.5$, because according to analyses based on the mean optical/mid-IR ratios of the sources, the sample is virtually 100% spectroscopically complete down to this redshift (La Franca *et al.* 2004). We have excluded all the AGN type sources. This left us with 148 redshift determined galaxies, 48 belonging to the deeper S1_R5 raster and the remaining 100 galaxies to the surrounding areas S1_Rest.

The angular distribution of ELAIS-S1 galaxies in our sample is displayed in Fig.1 (filled dots). The galaxy surface density is higher in the central region corresponding to the deeper S1_R5 raster.

The continuous line histograms in both panels of Fig. 2 shows the redshift distribution of the ELAIS-S1 galaxies in the S1_R5 (top) and S1_Rest (bottom) rasters. Gonzalez-Solares *et al.* (2004) have shown that the redshift distribution of ELAIS objects obtained from follow-up spectroscopic observations and photometric redshifts is consistent with that predicted from the ELAIS luminosity function of Pozzi *et al.* (2004). This redshift distribution will be used in the next section to estimate the galaxy correlation function and to construct the mock ELAIS catalogs.

¹ Data and related papers about the ELAIS southern survey are available at: <http://www.fis.uniroma3.it/~ELAIS>

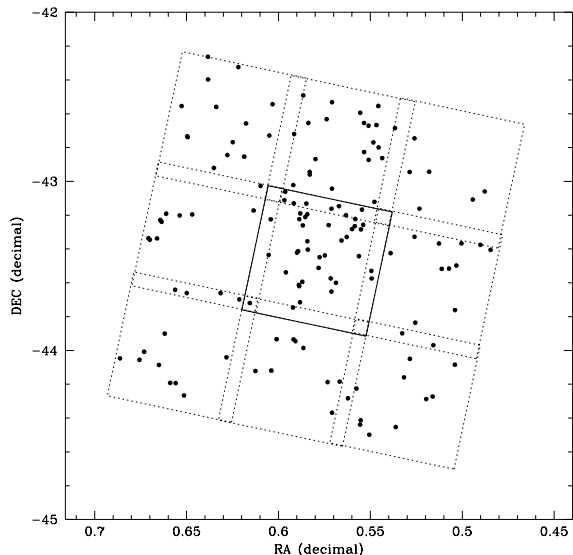


Figure 1. The angular distribution of ELAIS-S1 sources. The solid square is the central raster S1_R5, observed three times.

3 MEASURING THE REDSHIFT SPACE CORRELATION FUNCTION $\xi(s)$

Our purpose is to estimate the redshift-space two point correlation function of ELAIS-S1 galaxies and its uncertainties. It is worth stressing here that clustering in redshift-space is systematically different from the true one in real-space. On small scale, velocity dispersion in virialized systems smears out structure along the line of sight, hence depressing the amplitude of $\xi(s)$ at small separation. On large scales, coherent infall motions in high density regions or outflows from low density environments enhance structure along the line of sight and thus increase the amplitude of $\xi(s)$ on the corresponding scales. Here we make no attempt of correcting for redshift-space distortions. Therefore, direct comparisons will only be made with similar measurements of the redshift-space two point correlation function of other galaxy redshift catalogs.

3.1 Estimate of $\xi(s)$

Several different methods have been proposed to estimate the two point correlation function. In this work we use the Landy & Szalay (1993) [LS] estimator that, according to extensive numerical tests, turned out to be the best suited for astrophysical applications (Kerscher, Szapudi and Szalay 2000).

With the LS estimator a reliable and unbiased estimate of $\xi(s)$ is obtained by cross-correlating the real dataset with a sample of fake objects lacking any spatial correlation which, however, suffers from the same selection effects and incompleteness of the real catalog. To obtain a sample of synthetic objects we first create a random sample of points uniformly distributed over the same area as the real dataset, and then we generate their redshift distribution constrained to match that of the real objects determined by Pozzi *et al.*

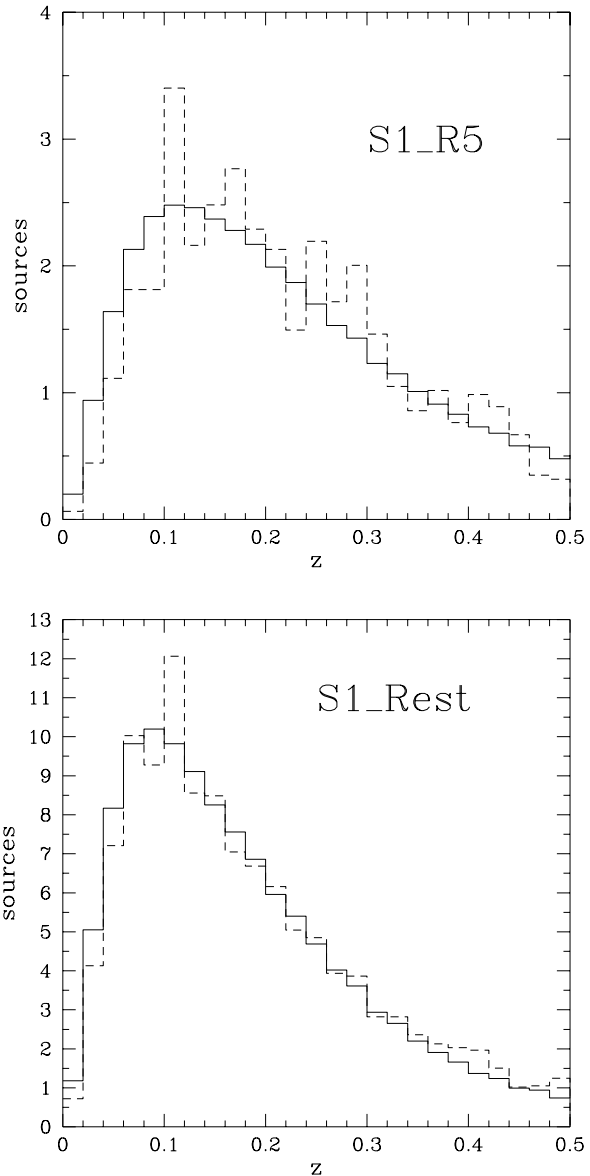


Figure 2. The redshift distribution of the sources in the S1_R5 raster (top panel) and in S1_Rest (bottom panel). The solid lines histogram indicates the redshift distribution of galaxies in the real ELAIS-S1 sample, while the dashed-line histogram indicates the average redshift distribution of objects in the 30 mock ELAIS-S1 catalogs.

(2004). For each random catalog we generate 10 times the number of fake objects as real galaxies.

The LS estimator is:

$$\xi(s) = \frac{N_{DD}(s)}{N_{RR}(s)} \left(\frac{n_R}{n_D} \right)^2 - 2 \frac{N_{DR}(s)}{N_{RR}(s)} \left(\frac{n_R}{n_D} \right) + 1, \quad (1)$$

where N_{DD} , N_{DR} and N_{RR} as the weighted data-data, data-random and random-random pair counts with redshift-space separation s . n_D and n_R are the mean densities of galaxies and random objects, respectively.

The flux limited nature of our dataset is accounted for by weighting each galaxy by

$$w_i = \frac{1}{1 + 4\pi n(z_i)J_3(s)}, \quad (2)$$

where $n(z_i)$ is the observed space density of galaxies at redshift z_i and $J_3(s) = \int_0^s \xi(r)r^2 dr$ (Efstathiou 1988). To implement this weighting scheme, that requires prior knowledge of $\xi(s)$, we have adopted an iterative procedure in which we first compute $\xi(s)$ using $w_i = 1$ and then we fit a power law to the results in the range $1 - 10 h^{-1}\text{Mpc}$. Then we compute the new weights w_i by truncating the maximum value of J_3 to 1500. Only one iteration was needed to obtain a stable result.

To check the robustness of our results we have varied both the estimator of $\xi(s)$ and the weighting scheme. More precisely, we have also used the estimators of Hewett (1982), Davis & Peebles (1983) and Hamilton (1993). Moreover, for the case of the LS estimator only, we have implemented two alternative weighting schemes: the case of no weight (i.e. $w_i = 1$) and the case in which we weight by the inverse of the selection function (i.e. $w_i = n_D/n(z_i)$). In all cases explored we have found that the various estimates of $\xi(s)$ were consistent, within the errors, in the range $1 - 10 h^{-1}\text{Mpc}$.

3.2 Errors estimation

To quantify the uncertainties in the estimate of $\xi(s)$ we have measured the correlation function in a sets of 30 independent mock galaxy catalogs designed to mimic the properties of the real ELAIS-S1 sample.

These mock catalogs were constructed from the N-body numerical experiment labelled L3S performed by Cole *et al.* (1998). Their simulation assumes a flat ΛCDM model cosmology with $\Omega_m = 0.3$, $\Lambda = 0.7$ an rms fluctuation of the mass contained in spheres of radius $8 h^{-1}\text{Mpc}$, $\sigma_8 = 1.13$ and a CDM power spectrum with shape parameter $\Gamma = 0.25$. The simulation box side is $345.6 h^{-1}\text{Mpc}$ and has 192^3 particles.

To construct each mock catalog we have used three different output of the simulations (corresponding to redshifts $z=0$, $z=0.33$ and $z=0.5$) and took advantage of the periodic boundary conditions to obtain different configurations of points in each box by re-centering the coordinate system on a particle chosen at random. We have then stacked six boxes in order of increasing redshift (three of them at $z=0$, two at $z=0.33$ and one at $z=0.5$), placed the observer at the center of the first box and identified the X coordinate with the direction of stacking. We have then identified the direction of the X axis with the center of the ELAIS field and considered all particles within an area of $2 \times 2 \text{ deg}^2$ from the field centre. To assign each particle a redshift we have used the distance to redshift relation for a flat, ΛCDM universe

$$r = \frac{c}{H_0} \int_0^z \frac{dz'}{\sqrt{\Omega_m(1+z')^3 + \Omega_\Lambda}}, \quad (3)$$

where r is the comoving distance, and then added the line of sight component of the particle peculiar velocity. Finally, a population of mock galaxies have been extracted from the particles through a Montecarlo rejection procedure designed to match the observed redshift distribution of real ELAIS galaxies in both the inner $40 \times 40 \text{ arcmin}^2$ S1_R5-like, and the outer S1_Rest-like samples. This procedure has been repeated to obtain 30 mock ELAIS-S1 samples, containing

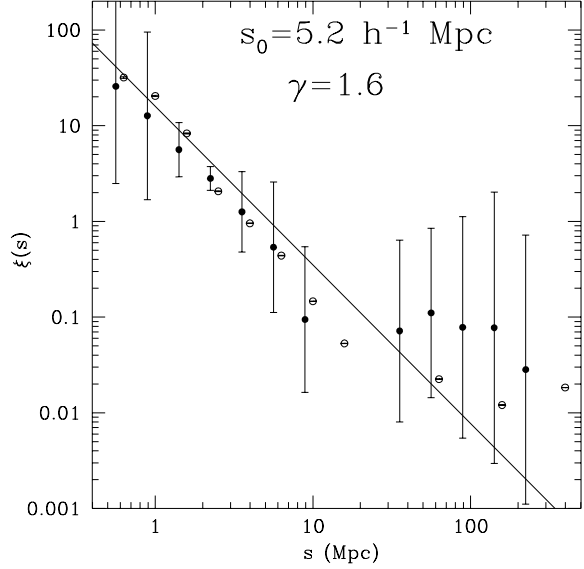


Figure 3. Average $\xi(s)$ measured in the 30 mock ELAIS-S1 catalogs (filled dots) and the rms scatter around the mean (errorbars). Open dots shows the “true” $\xi(s)$ of all particles in the simulation contained in a region with the same volume of the ELAIS-S1 sample. The straight line represents the best power law fit to the “true” $\xi(s)$ in the range $1 - 10 h^{-1}\text{Mpc}$. The values of the best fit parameters are also shown.

~ 120 objects each, for which we have evaluated the two-point correlation function. The mean redshift distribution of fake objects in the 30 catalogs is shown in of Fig. 2 (dashed line histogram) for the S1_R5 (top panel) and S1_Rest (bottom) rasters

The filled dots in Fig. 3 shows the average $\xi(s)$ in the 30 mock catalogs. The errorbars represent the rms scatter around the mean values. They constitutes our estimate of errors in the measurement of two point correlation function of the real ELAIS-S1 galaxies. These errors account for cosmic variance and sample noise, that constitutes the main source of uncertainty. The large size of the sample guarantees that the ‘integral constraint’ correction is only 5% (Gonzalez-Solares *et al.* 2004) and thus can be neglected in the error budget.

The open dots in Fig. 3 shows the “true” $\xi(s)$ of the simulation, measured by considering all particles in one of our ELAIS-like samples. The “true” $\xi(s)$ is consistent with the average $\xi(s)$ of the mocks, indicating that our method for estimating $\xi(s)$ is indeed unbiased.

The mock ELAIS-S1 catalogs mimic the geometry and selection effects of the real sample and account for the spatial clustering and its evolution in a flat ΛCDM universe. However, they are not guaranteed to reproduce the clustering properties of the ISO galaxies unless, of course, these trace the underlying mass density field out to $z = 0.5$.

As we have verified *a posteriori* this is indeed the case, in the sense that the “true” $\xi(s)$ in the range $1 - 10 h^{-1}\text{Mpc}$ is well approximated by a power law whose best fit parameters, displayed in Fig. 3 are consistent within the errors with those determined in the analysis of the real ELAIS-S1 sample presented in the following section.

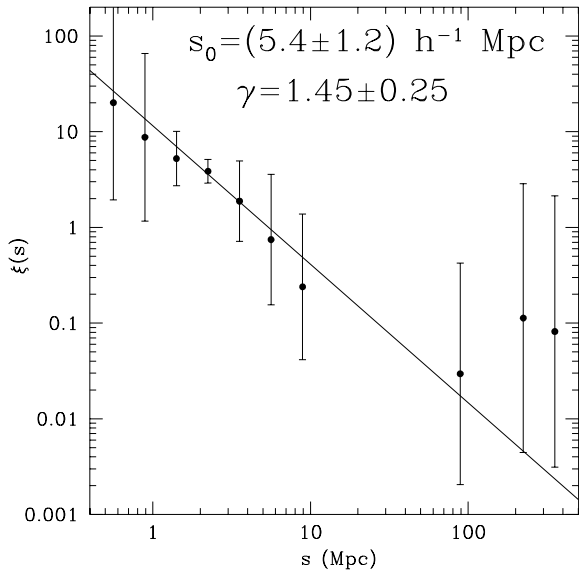


Figure 4. The redshift-space correlation function for the ELAIS-S1 galaxy sample (filled dots). Error bars have been calculated using the 30 ELAIS-like mock catalogs. The solid line represents the power law best fit $\xi(s) = (s/s_0)^{-\gamma}$ to the data in the range $1 - 10 h^{-1}\text{Mpc}$. The best fit parameters are indicated in the plot.

4 RESULTS

The filled dots plotted in Fig. 4 represent the two-point correlation function of the ELAIS-S1 galaxies computed using the LS estimator. The errorbars, evaluated from the 30 ELAIS-S1 mock catalogs, are the same shown in Fig. 3. Clearly, $\xi(s)$ is well approximated by a power law out to separations of $10 h^{-1}\text{Mpc}$. In the range $1 - 10 h^{-1}\text{Mpc}$ the best fit power law model $\xi(s) = (s/s_0)^{-\gamma}$, has a correlation length of $s_0 = 5.4 \pm 1.2 h^{-1}\text{Mpc}$ and a slope $\gamma = 1.45 \pm 0.25$, both determined at the 90% confidence level. Including the correlation of galaxy pairs at separation $s = 0.6 h^{-1}\text{Mpc}$, also shown in the figure, does not modify this result appreciably.

Breaking down the sample by redshift does not change results significantly either. Indeed, in the *local* sample composed by 82 objects at $z < 0.2$ $\xi(s)$ is still well approximated by a power law in the range $1 - 10 h^{-1}\text{Mpc}$ with best fit parameters $s_0 = 5.4 \pm 1.6 h^{-1}\text{Mpc}$ and $\gamma = 1.6 \pm 0.4$. These values agree with those found for the *distant* sample of 66 objects at $0.2 \leq z < 0.5$ for which we have found $s_0 = 5.1 \pm 1.6 h^{-1}\text{Mpc}$ and $\gamma = 1.4 \pm 0.4$.

Finally, we have verified that evaluating errors from 100 bootstrap realizations of the ELAIS-S1 sample rather than from the mock catalogs does not change significantly the results as the correlation length only decreases by $\sim 10\%$ and the slope becomes $\sim 4\%$ flatter.

5 DISCUSSION AND CONCLUSIONS

In this work we have evaluated the redshift-space two point correlation function of mid-infrared selected galaxies in the deep ($z \leq 0.5$) ELAIS-S1 catalog. We found a significant, positive correlation signal at separations $\leq 10 h^{-1}\text{Mpc}$,

where the two point correlation function is well approximated by a power law model $\xi(s) = (s/s_0)^{-\gamma}$ with a correlation length of $s_0 = 5.4 \pm 1.2 h^{-1}\text{Mpc}$ and a slope $\gamma = 1.45 \pm 0.25$, with errorbars referring to a 90% confidence level. These results have been obtained using the LS estimator for $\xi(s)$ and by evaluating the errors from a set of 30 mock ELAIS-S1 catalogs. These results are robust, in the sense that they do not change significantly when varying the method of estimating $\xi(s)$ (see section 3.1) or when using different strategies to assess the errors (sections 3.2 and 4).

It is interesting to compare our results with those obtained from similar analysis of galaxy clustering in redshift-space. Table 1 shows our result together with the corresponding results obtained from some of the major galaxy redshift surveys, characterized by their pass-band/wavelength of selection (column 2) and the redshift ranges they cover (column 3). It is worth stressing that deviations of the two point correlation function from a pure power law shape are more serious in redshift-space than in real-space, making it difficult to compare results obtained from the analyses of different galaxy samples. To ensure a fair comparison, all best fit parameters listed in columns 4 and 5 of Table 1 refer to ranges of separations where all measured $\xi(s)$ are well approximated by a power law. These ranges turned out to be very close to that of $[1 - 10] h^{-1}\text{Mpc}$ considered in our analysis, although some of the parameters in the Table have been obtained by pushing the estimate of $\xi(s)$ down to scale as small as $0.1 h^{-1}\text{Mpc}$ (the 2dFGRS case) or up to separations as large as $16.4 h^{-1}\text{Mpc}$ (as in the case of the LCRS sample).

Our results are fully consistent with those obtained from the analysis of the PSCz survey (Hawkins *et al.* 2001), that consists of $\sim 15,000$ *IRAS* galaxies selected at $60\mu\text{m}$, i.e. in a mid-infrared band similar to that of ELAIS galaxies. This sample is, however, much more local than ours and thus the agreement between the two results indicates that the clustering properties of mid-infrared selected objects do not evolve significantly between $z = 0$ and $z = 0.3$. This conclusion is corroborated by the consistency found between the two measurements of $\xi(s)$ performed in the *local* ($z < 0.2$) and *distant* ($0.2 \leq z < 0.5$) ELAIS-S1 subsamples. Unfortunately, the large uncertainties in our estimate of $\xi(s)$, that mainly result from the sparseness of the ELAIS-S1 galaxy catalog, do not allow to set strong constraints on the clustering evolution.

The lack of significant evolution in the ELAIS galaxy clustering has already been noticed by Gonzalez-Solares *et al.* (2004). In their analysis, that consisted in deprojecting the angular correlation function of ELAIS galaxies via Limber equation, they have measured a real-space two point correlation function with a slope ($\gamma = 2.04 \pm 0.18$) and a correlation length ($r_0 = 4.3^{+0.4}_{-0.7} h^{-1}\text{Mpc}$) that are fully consistent with those measured in the PSCz catalog ($\gamma = 2.04 \pm 0.18$ and $r_0 \approx 3.7 h^{-1}\text{Mpc}$, Jing, Börner & Suto (2002)). It is worth stressing that difference between our result and that of Gonzalez-Solares *et al.* (2004) originates from systematic redshift space distortions that affect our analysis and result in a shallower slope and a larger correlation length of the two point-correlation function.

Focusing on the mid-infrared objects is of considerable interest since they trace the underlying mass distribution in the local universe. The consistency that we have found

Table 1. Clustering of Different Galaxy Redshift Surveys: the Parameters of the Power Law Model

Survey	Selection Band	Δz	$s_0 (h^{-1} \text{Mpc})$	γ
ELAIS-S1 ¹	15 μm	0.0-0.5	5.40 ± 1.20	1.45 ± 0.25
PSCz ²	60 μm	0.004-0.1	4.77 ± 0.20	1.30 ± 0.04
CfA2 ³	B-band	0.0-0.05	~ 7.5	~ 1.6
ORS ⁴	B-band	0.0-0.027	7.60 ± 1.20	1.60 ± 0.10
LCRS ⁵	R-band	0.033-0.15	6.3 ± 0.3	1.86 ± 0.03
SDSS ⁵	r^* -band	0.019-0.13	~ 8.0	~ 1.2
2dFGRS ⁶	b_j -band	0.01-0.20	6.82 ± 0.28	1.57 ± 0.07

¹This analysis²Hawkins *et al.* (2001)³de Lapparent, Geller & Huchra (1988)⁴Hermit *et al.* (1996)⁵Tucker *et al.* (1997)⁶Zehavi *et al.* (2002)⁷Hawkins *et al.* (2003)

between the $\xi(s)$ in the real sample and the one measured in our mock ELAIS-S1 catalogs in which galaxies are identified with the particles of the parent N-body simulation, suggests that mid-infrared selected galaxies are indeed almost unbiased tracers of the underlying mass density field out to $z = 0.5$.

It is interesting to compare our results with those obtained using optically-selected galaxy samples, some of which is listed in Table 1. We confirm the well known fact that infrared selected objects are significantly less clustered than optical galaxies, although the discrepancy depends on the depth of the sample and (mainly) on the selection band, being larger for SDSS, r^* selected objects than for 2dF galaxies selected in the b_j band.

Investigating how this discrepancy change with redshift, i.e. how the relative clustering of different objects evolve with time, is of fundamental importance since it will allow to cast light on the galaxy formation and evolution processes. While this work constitutes an early step in this direction, strong observational constraints for theories of galaxy evolution will only be obtained by extending and improving samples like ELAIS-S1, which implies carrying out larger and deeper infrared redshift surveys like that already planned in the SWIRE programme (Lonsdale *et al.* 2003).

ACKNOWLEDGEMENTS

EB and FLF acknowledge ASI, INAF and MIUR (under grant COFIN-03-02-23) for financial support.

REFERENCES

- Adelberger, K.L., 2003, ApJ, 584, 45
 Coil, A. *et al.*, 2004, ApJ, 609, 525
 Cole, S., Hatton, S., Weinberg, D.H. & Frenk, C.S., 1998, MNRAS, 300, 945
 Davis, M., & Peebles, P.J.E., 1983, ApJ, 267, 465
 Davis, M. *et al.*, 2003, Proc. SPIE, 4834, 161
 Efstathiou, G., 1988, in Lawrence A., ed., Proc. 3rd *IRAS* Conf., Comets to Cosmology, Springer, New York, p. 312
 de Lapparent, V., Geller, M.J. & Huchra, J.P., 1988, ApJ, 332, 44
 Gonzalez-Solares, A.E., *et al.*, 2004, MNRAS, 352, 44
 Gruppioni, C. *et al.*, 2002, MNRAS, 335, 831
 Gruppioni, C. *et al.*, 2005, ApJ, 618, L9
 Hamilton, A.J.S., 1993, ApJ, 417, 19
 Hawkins, E., Maddox, S., Branchini, E., Saunders, W., 2001, MNRAS, 325, 589
 Hawkins, E., *et al.* 2003, MNRAS, 346, 78
 Hermit, D.L. *et al.* 1996, MNRAS, 283, 709
 Hewett, P.C., 1982, MNRAS, 201, 867
 Jing, Y.P., Börner, G. & Suto, Y., 2002, ApJ, 564, 15
 Kerscher, M., Szapudi, I., & Szalay, A.S., 2000, ApJL, 535, 13
 Kessler, M.F. *et al.* 1996, A&A, 315, L27
 La Franca, F. *et al.* 2004, AJ, 127, 3075
 Lahav, O. *et al.* 2002, MNRAS, 333, 961
 Landy, S.D. & Szalay, A.S., 1993, ApJ, 412, 64
 Lari, C. *et al.*, 2001, MNRAS, 325, 1173
 Lonsdale, C.J. *et al.*, 2003, PASP, 115, 897
 Magdwick, D.S. *et al.*, 2003, MNRAS, 344, 847
 Matute, I. *et al.* 2002, MNRAS, 332, L11
 Norberg, P. *et al.*, 2002, MNRAS, 332, 827
 Oliver, S. *et al.*, 2000, MNRAS, 316, 749
 Pozzi, F. *et al.*, 2004, ApJ, 609, 122
 Rowan-Robinson, M. *et al.* 2004, MNRAS, 351, 1290
 Serjeant, S. *et al.* 2000, MNRAS, 316, 768
 Szapudi, I., Branchini, E., Frenk, C.S., Maddox, S., Saunders, W., 2000, MNRAS, 318, L45
 Taylor A. N., Ballinger W.E., Heavens A.F. & Tadros H., 2002, MNRAS, 327, 689
 Tegmark M., Zaldarriaga M., & Hamilton A.J., 2001, Phys. Rev. D, 67, 3007
 Tucker, D.L. *et al.* 1997, MNRAS, 285, L5
 Vanzella, E. *et al.* 2004, astro-ph/0406591

Verde, L. *et al.* 2002, MNRAS, 335, 432
Wirth, G.D. *et al.* 2004, AJ, 127, 3121
Zehavi, I. *et al.* 2002, ApJ, 571, 172